Strain relaxation kinetics in $Si_{1-x}Ge_x$/Si heterostructures

R. J. Hauenstein, B. M. Clemens,[a] R. H. Miles, and O. J. Marsh
Hughes Research Laboratories, Malibu, California 90265

E. T. Croke and T. C. McGill
California Institute of Technology, Pasadena, California 91125

Strain relaxation in $Si_{1-x}Ge_x$/Si superlattices and alloy films is studied as a function of *ex situ* anneal treatment with the use of x-ray diffraction and Raman spectroscopy. Samples are grown by molecular-beam epitaxy at an unusually low temperature (≈ 365 °C). This results in metastably strained alloy and superlattice films significantly in excess of critical thicknesses previously reported for such structures. Significant strain relaxation is observed upon anneal at temperatures as low as 390 °C. After a 700 °C, 2 h anneal, superlattices are observed to relax less fully ($\sim 43\%$ of coherent strain) than corresponding alloys ($\sim 84\%$ of coherent strain). Also, the strain relaxation kinetics of a $Si_{1-x}Ge_x$ alloy layer is studied quantitatively. Alloy strain relaxation is approximately described by a single, thermally activated, first order kinetic process having activation energy $E_a = 2.0$ eV. The relevance of our results to the microscopic mechanisms responsible for strain relaxation in lattice-mismatched semiconductor heterostructures is discussed.

I. INTRODUCTION

Recently, it has been shown[1-3] that, through molecular-beam epitaxy (MBE), a coherently strained $Si_{1-x}Ge_x$/Si heterostructure can be grown on Si to a thickness significantly in excess of the critical thicknesses h_c predicted by thermodynamic equilibrium theories.[4,5] Since then, it has been directly demonstrated for $Si_{1-x}Ge_x$/Si strained layer superlattices (SLS) that the onset of strain relaxation is dependent on growth temperature.[6,7] The above results imply the existence of a kinetic barrier to strain relaxation which is significant at typical MBE growth temperatures, and which allows the growth of *metastable* structures in excess of the equilibrium h_c. In addition, other work[8] has shown that the *extent* of strain relaxation apparently differs for SLS structures and equivalent single $Si_{1-x}Ge_x$ alloy films on Si due to the effects of microstructural details on the strain relaxation process. Both the extent and the kinetics of strain relaxation are dependent upon the actual mechanisms which are responsible for strain relaxation. Several possible strain relaxation mechanisms have been proposed.[8-10] Unfortunately, neither the actual mechanisms are accurately known, nor has strain relaxation on any given bulk sample been followed in sufficient detail.

In this paper, we investigate the relaxation of coherent strain in highly metastable $Si_{1-x}Ge_x$ alloy films and superlattices. The extreme metastability of the structures is due to a "freezing in" of the coherent strain through MBE growth at an unusually low temperature (≈ 365 °C). Such samples relax appreciably (up to $\sim 84\%$ of the coherent strain) upon *ex situ* anneal treatment. The strain relaxation of the metastable structures is studied quantitatively after successive *ex situ* anneals at fixed times for various temperatures with the use of x-ray diffraction (XRD) and Raman spectroscopy.

The experimental details of this work are summarized in Sec. II. There, we describe the sample set used in this study. Of particular note is the fact that all of the samples, both

alloys and superlattices, were designed to have the same average properties, i.e., the same total thickness (≈ 5000 Å) and average Ge molar fraction ($\bar{x} \approx 20\%$) while at the same time differing significantly in their detailed structure. This is to facilitate comparison among samples of the strain relaxation, which is presumed to be driven by factors depending on average properties such as excess stress,[10] but hindered by microstructural features such as periodic internal strain fields.[8]

Our results are discussed in Sec. III and IV. The results directly demonstrate the existence of a thermal activation barrier to strain relaxation in both single alloy layers and superlattices. Alloy samples which are initially coherently strained are seen to relax their strains to a greater extent than the corresponding superlattices. The superlattices are seen to relax commensurately, i.e., as a whole with respect to the substrate rather than layer by layer. A more extensive set of measurements on one of our alloy samples shows strain relaxation to be given approximately by a first order kinetic process. For this sample, we obtain an activation energy E_a of 2.0 eV. Finally, our conclusions are given in Sec. V.

II. EXPERIMENTAL

A. MBE growth

The samples used in this study were grown in a new Perkin–Elmer model 430S Si MBE system. Codeposition of Si and Ge took place in an ultrahigh vacuum (UHV) chamber (base pressure $< 10^{-10}$ Torr) from dual *e*-beam evaporation sources onto rotating, heated, 3 in. Si (100) substrates. Si and Ge fluxes were simultaneously sensed and feedback stabilized with the use of a cathodoluminescent flux sensor (Inficon, Sentinel III). A nominal Si deposition rate of 1.0 Å/s was employed, along with the appropriate Ge deposition rate needed to achieve the desired alloy stoichiometry in the

TABLE I. $Si_{1-x}Ge_x/Si$ sample characteristics. Average alloy compositions $\bar{x}$ were determined by Auger electron spectroscopy for samples SL1 and SL2 ($\pm 1\%$), and by x-ray diffraction for the remaining samples ($\pm 0.5\%$).

Sample	$\bar{x}(\%Ge)$	$t(\text{Å})$	Type	Nominal structure
SL1	22%	5110	Superlattice	$Si_{0.4}Ge_{0.6}$/Si (70 Å/140 Å)×24
SL2	22%	5180	Superlattice	$Si_{0.7}Ge_{0.3}$/Si (140 Å/70 Å)×24
SL3	20%	5220	Superlattice	$Si_{0.6}Ge_{0.4}$/Si (72 Å/73 Å)×36
A1	23%	5000	Alloy	...
A2	21%	5000	Alloy	...

$Si_{1-x}Ge_x$ layers. Substrates were heated radiatively with a graphite-filament heater, and temperature was monitored and controlled with a thermocouple and a proportional–integral–derivative controller/programmer (Micristar model 828D). True substrate versus thermocouple temperature was calibrated with the aid of an optical pyrometer (Ircon, W-series) and through in situ observation of Si–Al and Si–Au eutectic reactions to an estimated absolute accuracy of ± 20 °C.

Prior to loading into vacuum, the Si substrates were degreased, dipped into an HF solution, and rinsed in deionized water. Samples were then immediately loaded into the MBE system. In situ surface preparation consisted of thermal oxide desorption near 850 °C assisted by a slight Si flux.[11,12] This process was continued for $\sim$1–2 min until a Si (2×1) reconstructed surface was observed in reflection high-energy electron diffraction (RHEED). At this point, the temperature was lowered to $\sim$700 °C and a 1000–2000-Å-thick Si buffer layer was grown to ensure an atomically clean starting surface for growth of subsequent heteroepitaxial layers.

The samples grown for this study are summarized in Table I. These consist of three superlattice (SL1–SL3) and two alloy samples (A1, A2). All samples have a heteroepitaxial layer thickness near 5000 Å and an average Ge content near 20%. As indicated in Fig. 1, these characteristics place all of the samples in the "relaxed" region of the empirical critical thickness curve of People and Bean,[2] which is based on $Si_{1-x}Ge_x$ alloy growth on Si near 550 °C. However, our alloy and superlattice layers were all grown at an unusually low temperature ($\approx$365 °C) to form metastably strained films. Despite our unusually low growth temperature, most of the present structures are seen to be of very high structural quality as judged by high-resolution x-ray diffraction and transmission electron microscopy (TEM). As we shall see below, the low growth temperature did indeed result in attainment of full coherent strain in most of our samples.

B. Ex situ anneal

The samples were annealed in a conventional quartz tube diffusion furnace under a flowing N_2 gas ambient. Closed-loop temperature control was used to provide repeatability of ± 1 °C, and anneal temperatures were independently monitored by means of a thermocouple inserted into the furnace. All samples were quickly loaded onto a prewarmed quartz boat and Si bed to minimize errrors due to warmup temperature transients. Similarly, after each anneal step the samples were brought quickly to room temperature by quenching in water. The transient temperature response involved in the above procedures was studied in detail, and a slight systematic correction was applied to the final results presented below in Fig. 7 (though this correction does not alter the value obtained for E_a).

C. Strain measurements

Quantitative measurements of epilayer strains was accomplished with the aid of XRD and Raman spectroscopy. The XRD measurements consisted of θ–2θ scans of the symmetric (400) Bragg reflections of the substrate and heteroepitaxial layers. In the case of simple $Si_{1-x}Ge_x$ layers this results in a single x-ray peak while in the case of superlattices a family of peaks is observed. Strain is determined directly from the peak positions of the epilayer and substrate. For this measurement we used a powder diffractometer (Philips) with a Cu-anode x-ray source. Cu K_β rather than Cu K_α radiation was selected with the aid of a graphite monochro-
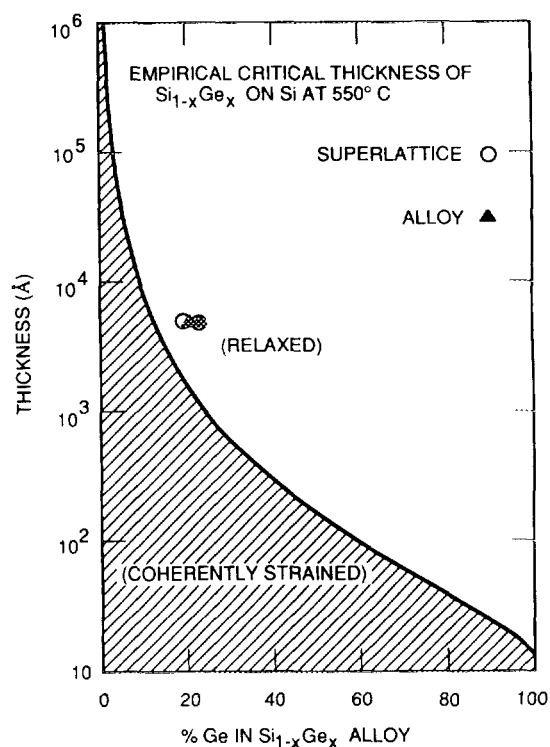
FIG. 1. Sample set for the present experiments. $Si_{1-x}Ge_x$ single layers and superlattices were grown as indicated. Unusually low-temperature (365 °C) MBE growth permits growth of nearly fully coherently strained structures despite the fact that the samples are in the relaxed region of the graph.

mating filter to avoid the need for Rachinger correction of the scans due to the Cu K_α doublet. Data scans were acquired digitally and peak positions (in 2θ) were numerically determined using the second-derivative minimization technique to an estimated uncertainty of $\pm$ 0.005°.

Raman spectroscopy was also used to measure strain through observation of strain-induced shifts in optical phonons. In this case, a backscattering geometry was employed. Unpolarized light from an Ar$^+$-ion laser (λ_L = 4765 Å) was allowed to impinge onto the sample at room temperature near normal incidence. The unpolarized, Raman-scattered Stokes lines were collected along the substrate normal direction with the use of a double-pass grating spectrometer (SPEX, model 1404) and a liquid-nitrogen-cooled photomultiplier tube. Again, scans were acquired digitally and peak positions determined numerically by the procedure mentioned above for the x-ray data. Estimated Raman peak position uncertainty is $\pm$ 0.1 meV. At the laser wavelength used, all of the incident light is absorbed in (hence, all of the Raman signal comes from) the epitaxial layers.

III. RESULTS

A. Extent of strain relaxation

Initially, we annealed pieces of all of our samples together at 700 °C for 2 h to examine the extent of strain relaxation. This thermal treatment was seen to be more than adequate to allow complete strain relaxation while avoiding noticeable interdiffusion. Additionally, we note that any strain due to differential thermal expansion at this temperature is quite negligible ($\sim 10^{-2}\%$) in comparison with the lattice mismatch. Figure 2 shows XRD scans of an alloy and a superlattice sample before and after the anneal. The peaks that are indicated in the figure correspond to the Si$_{1-x}$Ge$_x$ alloy (400) reflection in the upper curves, and to the (400)-like zeroth-order superlattice reflection in the lower curves. The x-ray peaks shown for the alloy sample correspond to atomic plane spacings along the substrate normal direction. The interplanar distance d is simply related to the peak position 2θ through Bragg's law,

$$\lambda = 2d \sin \theta. \tag{1}$$

The d-spacings, and hence peak positions, are fixed by both alloy comparison and strain. For an *unstrained* Si$_{1-x}$Ge$_x$ alloy of Ge molar fraction x the d-spacing is given approximately by Vegard's law as

$$d_x^{\text{rlx}} = d_{\text{Si}} [1 + (4.18\%)x], \tag{2}$$

where d_{Si} = 1.358 Å is the spacing between adjacent bulk Si (400) planes, and the bulk lattice constant mismatch between Si and Ge is 4.18%. In contrast, for a *coherently strained* alloy, the d-spacing, due to tetragonal distortion[1] ϵ_T is

$$d_x^{\text{coh}} = d_x^{\text{rlx}} [1 + (4.18\%)x\epsilon_T]$$

$$\approx d_{\text{Si}} [1 + (4.18\%)(1 + \epsilon_T)x], \tag{3}$$

where ϵ_T is equal to 0.76 for alloy compositions studied here.[13] For superlattices, the interpretation of x-ray data is similar except that in this case we analyze the position of the
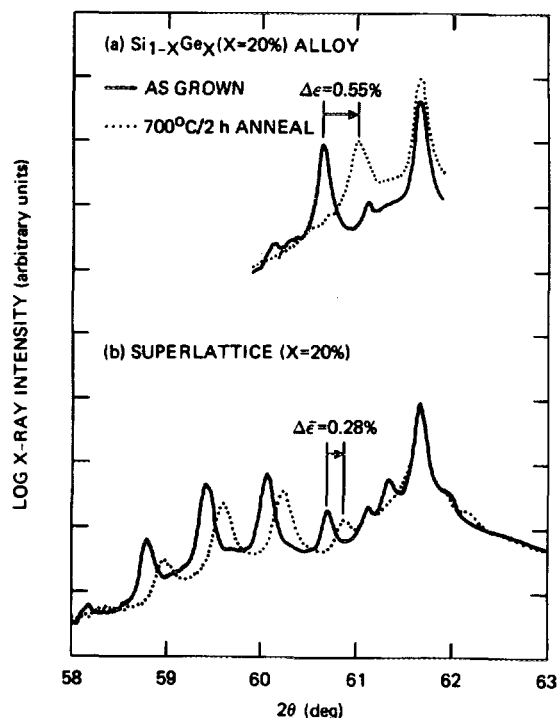

FIG. 2. X-ray (θ–2θ) spectra showing strain relaxation in alloy sample A2 (a) and superlattice SL3 (b). The symmetric Bragg (400) alloy peak and (400)-like zeroth-order superlattice peaks, before and after the anneal, are indicated. The alloy relieves about 84% of its coherent strain while the superlattice loses only about 43% ($\pm$ 2% absolute error). The large peaks at 61.68° are due to the Si substrate.

zeroth order superlattice peak, and we replace x by $\bar{x}$ and d by $\bar{d}$, the *average* composition and d-spacing in the superlattice, respectively, in the above equations.

Considering the solid curves in Fig. 2, we see that before the anneal the alloy peak (sample A2) and zeroth-order superlattice peak positions (sample SL3) are the same. This is the peak position expected for a Si$_{0.8}$Ge$_{0.2}$ layer coherently strained to Si(100). From Table I we see that the average compositions of these two samples is approximately the same (20%). Thus, both samples are initially coherently strained as grown, according to the XRD measurement. After the anneal, the alloy peak is shifted toward increasing 2θ (smaller d) values by an amount which corresponds to a reduction in d-spacing of (0.55%) d_{Si}. From Eqs. (2) and (3), this corresponds to a relaxation of $\sim 84\%$ of the coherent strain. In contrast, the same figure shows that the superlattice as a whole relaxes only about 43% of its initial strain. The large peaks at 61.68° correspond to the Si substrate (400) reflection and do not shift as a result of the anneal. Also, the small peaks seen in Fig. 2(a) are due to scattering of Cu $K_{\beta 2}$ radiation from the same (400) substrate and alloy reflections. In general, the relaxation of any strained film of finite thickness will be incomplete, the equilibrium condition being given by the lattice mismatch partially accommodated elastically through strain and partially accommodated plastically through formation of misfit dislocations. However, this does not account for the differing extent of relaxation of the alloy and superlattice shown in Fig. 2. Since both samples are of the same average composition and total thickness,

simple energy minimization considerations would predict the same relaxation behavior for both.[3]

Raman spectra showing the same superlattice sample before and after the anneal are shown in Fig. 3. The spectra shown contain four prominent peaks. The peaks near 37, 52, and 62 meV are attributed to Ge–Ge, Si–Ge, and Si–Si local vibrations in the $Si_{1-x}Ge_x$ layers of the superlattice while the highest energy peak is the zone-center optical phonon mode (64.5 meV) from the Si layers. For the backscattering geometry along [100] employed here, the influence of the lattice-mismatch-induced biaxial stress and resultant tetragonal distortion is to shift both the Si and Si–Si phonon peaks in energy in approximate accordance with the relation[8,14]

$$\epsilon_{\parallel}(\%) = -1.1 \times \delta E(\text{meV}), \tag{4}$$

where $\epsilon_{\parallel}$ is the Si ($Si_{1-x}Ge_x$) layer strain in the plane of the interface with respect to the unstrained lattice constant of Si ($Si_{1-x}Ge_x$). In deriving Eq. (4) it is assumed that strains parallel and perpendicular to the interface are related by

$$\epsilon_{\perp}/\epsilon_{\parallel} = -\epsilon_T. \tag{5}$$

Thus, from Eq. (4), we see that strain relaxation in the film corresponds to a reduction in phonon energy. This behavior is demonstrated in Fig. 3. There, we see that both the Si–Si and the Si zone-center phonons shift together upon annealing toward lower phonon energies by an amount 0.5 meV. Furthermore, through Eq. (4) we see that the magnitude of

strain change is the same for both the $Si_{1-x}Ge_x$ and Si layers of the superlattice. This indicates that the initially coherently strained superlattice is relaxing as a whole with respect to the substrate rather than layer-by-layer. If the latter were the case, we should expect only the $Si_{1-x}Ge_x$ peaks to shift toward lower energies upon annealing since the Si layers, coherently strained to the substrate as grown, would already be unstrained. Further evidence that the superlattice is coherently strained as grown comes from the fact that the Si zone-center phonon peak position occurs at 64.5 meV, which is also the position observed for bulk Si.

In Fig. 4 and Table II we compare the relaxation of coherent strain in all of our samples as determined by XRD and Raman spectroscopy. In this figure, 0% strain relaxation corresponds to complete coherent strain as given by Eq. (3), and 100% relaxation corresponds to the bulk, unstrained condition specified by Eq. (2). [A small correction to Eq. (2) was applied for the case of the superlattices to take into account the variation in elastic constants with alloy layer composition such that 100% relaxation corresponds to the appropriate *free-standing* superlattice configuration.] Nominally, all data points should lie on the dashed diagonal line in the figure, corresponding to identical strains measured by XRD and Raman techniques. In comparison with the XRD scans, we see from Figs. 2 and 3 that the amount of peak shift relative to peak width is much smaller in the Raman spectra, rendering quantitative analysis less precise for the latter. This uncertainty is reflected in the error bars shown in Fig. 4.

Samples A1 and SL3 are both seen to be coherently strained as grown. Upon anneal, a significantly greater extent of relaxation is observed for the alloy sample than for
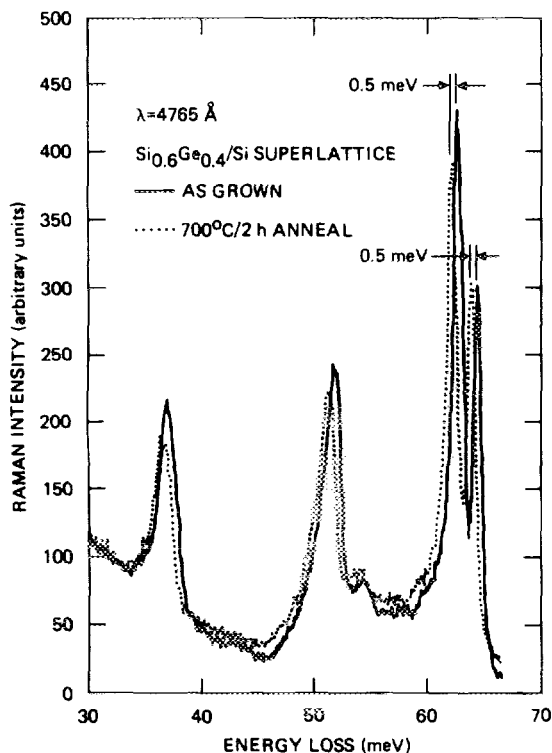

FIG. 3. Raman spectra of superlattice SL3 before and after the anneal. The peaks shown are all Stokes lines due to optical phonons. The highest energy peak (64.5 meV) is due to the Si layers of the superlattice. The peaks near 62, 52, and 37 meV are attributed to Si–Si, Si–Ge, and Ge–Ge local vibrations in the $Si_{1-x}Ge_x$ layers. The phonon peak shifts reveal that the Si and $Si_{1-x}Ge_x$ layers are relaxing commensurately. The shifts correspond to a strain change of ~0.6%, which is ~60% of the coherent strain.
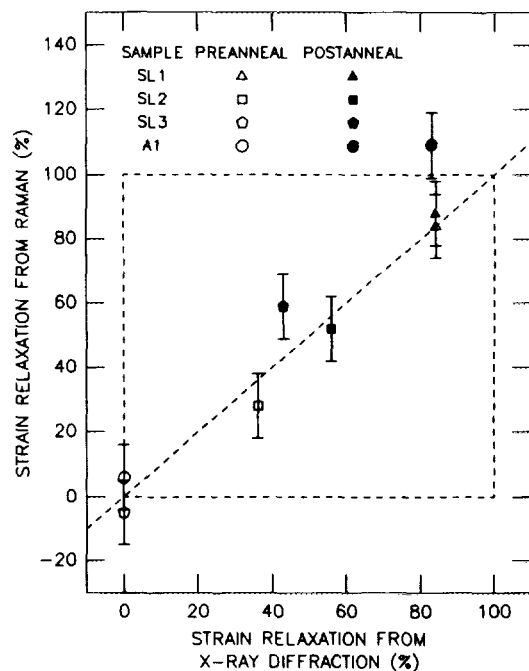

FIG. 4. Relaxation of coherent strain for superlattices and alloys as a result of a 700 °C/2 h anneal, determined by XRD and Raman spectroscopy. Open and solid symbols correspond to strain before and after the anneal, respectively. Superlattices relax less than the alloy shown. (No Raman is available for alloy sample A2, but XRD data agree with that shown here for alloy sample A1.)

TABLE II. Raw XRD and Raman data for samples before and after a 700 °C/2 h anneal, and the corresponding coherent strain relaxation, r. $\bar{\epsilon}_1^{xrd}$ is relative to the Si substrate. All stated uncertainties are given as absolute errors.

	Sample	$\bar{\epsilon}_1^{xrd}$ ($\pm 0.03\%$)	r^{xrd} ($\pm 2\%$)	E_{Si} (± 0.01 meV)	E_{Si-Si} (± 0.01 meV)	r^{Raman} ($\pm 10\%$)
Preanneal	SL1	0.97	84	63.6	61.0	84
Preanneal	SL2	1.36	36	64.2	62.8	28
Preanneal	SL3	1.44	0	64.5	62.8	− 5
Preanneal	A1	1.71	0	· · ·	63.4	6
Preanneal	A2	1.51	0	· · ·	· · ·	· · ·
Postanneal	SL1	0.97	84	63.6	60.9	88
Postanneal	SL2	1.22	56	64.0	62.6	52
Postanneal	SL3	1.16	43	64.0	62.3	59
Postanneal	A1	1.10	83	· · ·	62.5	109
Postanneal	A2	0.96	84	· · ·	· · ·	· · ·

the superlattice by both measurement techniques. Not shown in Fig. 4, but listed in Table II, is alloy sample A2, which, through XRD, is also observed to be coherently strained as grown, and to relax to the same extent as alloy sample A1 upon a similar anneal treatment. In contrast, superlattice samples SL1 and SL2 both appear to have relaxed during MBE growth. For example, SL1 is not seen to relax *at all* upon annealing in either XRD or Raman measurements, within experimental error. Comparison of the observed superlattice XRD scan with a simulation calculated in the kinematical approximation suggests that superlattice SL1 was fully relaxed as grown. As noted earlier, for a film of finite thickness there will always remain some residual strain in the "fully relaxed" state. In Fig. 4, this corresponds to a strain relaxation value less than 100%. We see both before and after the anneal that superlattice SL1 has relaxed ~ 84% of the full coherent strain for this structure. Interestingly, this strain relaxation value is nearly identical to that of alloy samples A1 and A2 after the anneal. Lastly, we see that superlattice SL2 appears to be ≈ 36% relaxed as grown from the XRD measurement, and subsequent to the anneal becomes ≈ 56% relaxed. This final relaxation state is similar to that of SL3. Thus, we see that, of the three superlattice and two alloy samples studied, all of the alloys relax to a significantly greater extent than the superlattices, except for the one superlattice that was already fully relaxed as grown. In the latter case, the final strain state of the superlattice is that of the fully relaxed alloy.

B. Alloy strain relaxation kinetics

In the preceding discussion we examined the extent of strain relaxation which results from a 700 °C, 2 h anneal treatment. We now consider the kinetics of strain relaxation for the case of a coherently strained $Si_{1-x}Ge_x$ alloy on Si (100). To accomplish this, we follow the partial relaxation of the alloy through a series of successive isochronal anneal steps at fixed temperatures ranging from 390 to 450 °C. These temperatures are significantly lower than the MBE growth temperatures typically employed elsewhere[1,8,15] (500–600 °C). For a fixed anneal temperature, the strain is observed to decay approximately exponentially in time to a residual strain value. Through comparison of decay rates at

different temperatures, we obtain an activation energy for the strain relaxation process.

Figure 5 shows x-ray scans taken on alloy sample A2 which was successively annealed at 414 °C in 35 min steps. The initial (coherent) and final (relaxed) states of the same sample are also shown for comparison. From the figure, we see that the alloy peak shifts in decreasing amounts with each successive anneal step. Also apparent is an initial broadening of the alloy peak (compare peaks labeled "COH" and "1"), after which successive anneals do not appear to result in significant further broadening. The initial broadening is probably due to the onset of dislocation generation in the film. Unfortunately, the resolution of the present measurements is too poor to permit a meaningful quantitative analysis of x-ray peak widths. This resolution can be
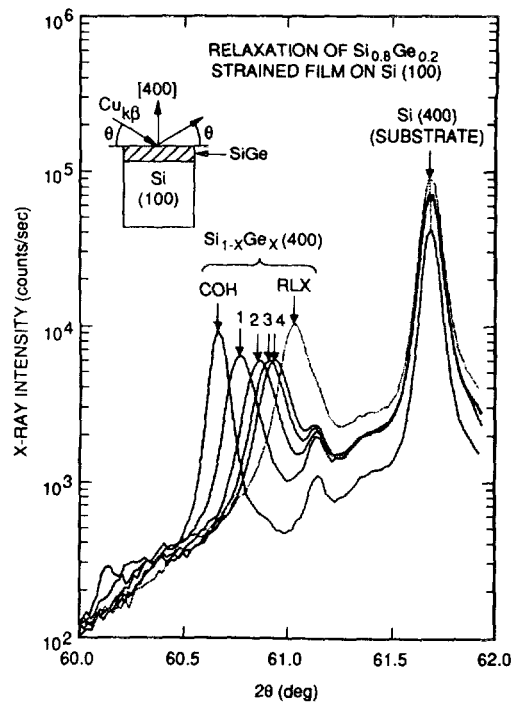

FIG. 5. θ–2θ XRD of alloy A2 as grown (COH), successively annealed at 414 °C/35 min (1–4), and after achieving the residual strain value (RLX). The relaxation decays exponentially to the residual value.

seen by considering the Si substrate peak in Fig. 5, whose width is entirely due to instrumental resolution. However, we note here that high-resolution x-ray diffraction (HRXRD) measurements made on this sample prior to the anneal using a four-crystal monochromator show that the initial alloy peak width is quite sharp, broadened essentially only due to finite alloy layer thickness. This initial, intrinsic alloy peak width is below the instrumental resolution associated with the scans shown in Fig. 5. Hence, we believe the initial sample to be of high structural quality, and that significant degradation of the crystallinity (due to dislocation generation) evidently occurs at the beginning of the strain relaxation process.

The temporal dependence which is typical of the strain relaxation in our alloy films is shown in Fig. 6. In this case, relaxation of sample A1 is shown after several 25 min anneal steps at 407 °C. Plotted in the figure is the alloy XRD peak position versus anneal time. The "fraction of coherent strain," η, defined by the equation

$$d_x(\eta) \equiv d_{Si}[+ (4.18\%)(1 + \eta\epsilon_r)x], \tag{6}$$

varies linearly from 100% to 0% as the strain varies between the fully coherent and fully relaxed values according to Eqs. (3) and (2), respectively. The value η_0 is the residual fraction of coherent strain observed after the relaxation has evidently proceeded to completion. In Fig. 6, we plot $\ln(\eta - \eta_0)$ versus anneal time. The data approximately exhibit a decaying exponential behavior. From the slope, a strain relaxation rate is obtained. The error bars presented in the figure correspond to x-ray peak position uncertainty.
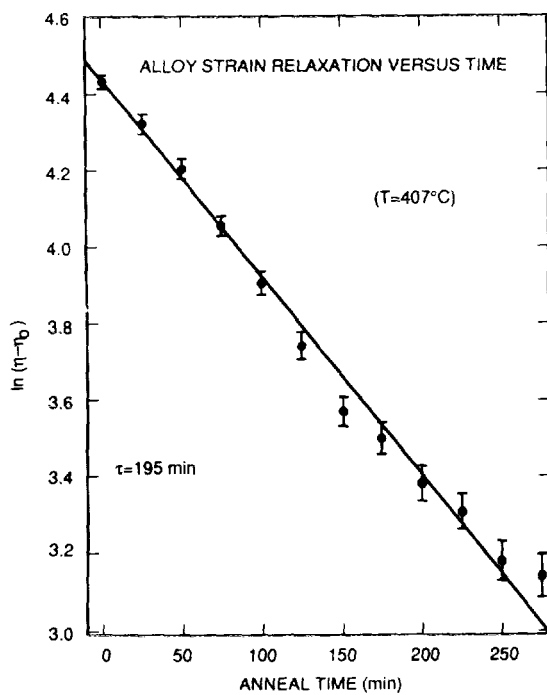
Despite the error bars, there appears to be a systematic deviation from a simple exponential decay, suggesting that the assumption of a single, first order kinetic process in only an approximation, and that the actual relaxation may be more complicated. That the relaxation is more complicated was also hinted at above in the discussion of peak broadening; for instance, the peaks appear to broaden quite nonlinearly with anneal time.

Figure 7 shows an activation energy plot of the strain relaxation of alloy sample A2. A slight systematic correction due to warmup transients in the anneal furnace (mentioned earlier in Sec. II) has been applied to the data. As noted above, this correction does not change the activation energy obtained. We see from the figure that the $Si_{1-x}Ge_x$ layer strain relaxation is approximately described by a single, thermally activated process. From the slope of the curve we obtain an activation energy for this sample of $E_a = 2.0 \pm 0.1$eV. The error bars shown in Fig. 7 are based on the statistical uncertainty of the relaxation rates obtained from data such as that shown in Fig. 6. As mentioned earlier, we estimate our anneal temperatures to be repeatable to ± 1 °C, though a slightly larger error in absolute temperature (no larger than ± 5 °C) is possible. The data points seen in Fig. 7 do not appear to exhibit a systematic deviation from the line. However, there does appear to be somewhat more scatter than would be expected from uncertainties in peak positions and temperatures alone. In fact, we take the observed scatter as further evidence that the assumption of a single, thermally activated description of strain relaxation is only approximately correct.
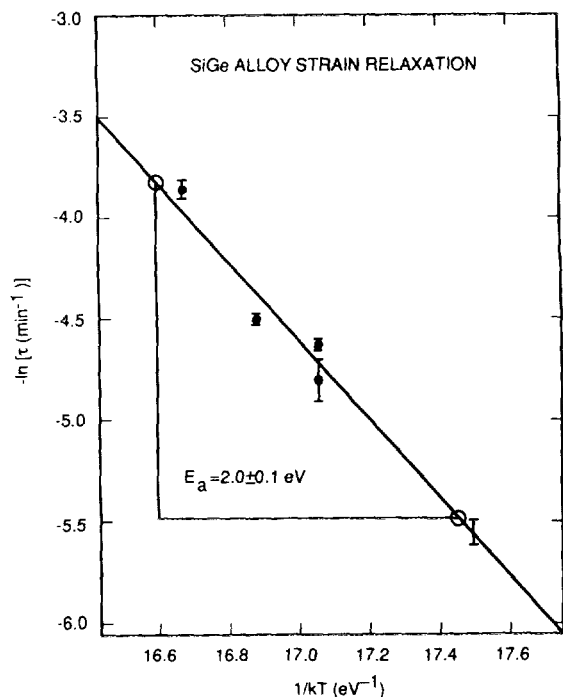

FIG. 6. Strain relaxation at fixed T for successive 25 min anneal steps. The parameter η is defined to vary linearly from 100% to 0% as the film strain varies between its theoretical fully coherent and fully relaxed values. The strain decays approximately exponentially in time. Because of the finite film thickness, a residual strain value $\eta_0 = 17\%$ is observed. The error bars are 1σ estimates due to uncertainty in x-ray peak positions.

FIG. 7. Activation energy plot of the strain relaxation rate vs anneal temperature for a $Si_{1-x}Ge_x$ alloy on Si. The activation energy is 2.0 ± 0.1 eV. The error bars are based on statistical uncertainty of relaxation rate estimated from plots of the type shown in the previous figure. The scatter of data points about the fit line suggests that the assumption of a simple, thermally activated description of strain relaxation is only approximately correct.

IV. DISCUSSION

We have shown in previous work[6,7] that, by lowering MBE growth temperature, superlattices could be grown coherently strained to thicknesses that are in excess of h_c values which were deduced[2] on the basis of MBE growth at the higher temperatrues (500–600 °C) commonly reported elsewhere,[1,8,15] and, further, that as the growth temperature is increased, a systematic strain relaxation is observed.[6,7] In the present work, we have likewise shown that it is possible to increase the empirical h_c for single $Si_{1-x}Ge_x$ layers through growth at reduced temperatures (≈ 365 °C) from the values deduced for growth near 550 °C,[1] and provide further evidence that: (i) growth of metastable strained $Si_{1-x}Ge_x/Si$ heterostructures is possible; (ii) empirical h_c is a function of MBE growth temperature; and (iii) strain relaxation is a thermally activated process. We have also seen that the nature of strain relaxation is dependent on more than the just average properties of the sample, as the positioning of a sample on a graph such as that shown in Fig. 1, even for the case of a growth temperature-dependent empirical critical thickness, might naively suggest. The question of whether or not a structure can be grown coherently strained, the extent of strain relaxation, and the rate of strain relaxation as well, depend on *detailed* as well as *average* structural characteristics.

To account for the observed phenomena, it is necessary to understand the driving force(s) responsible for strain relaxation, the mechanisms by which strain is relieved, and the dependence on the detailed heteroepitaxial structure. Energy minimization is clearly a driving force which depends on the average properties of the heteroepitaxial structure as a whole.[3] Since energy in a uniformly strained film is proportional to film thickness, at some point, it is energetically favorable for a strained film (or multilayered structure) to reduce its elastic strain energy at the expense of forming misfit dislocations. This is the basis of derivation of the so-called equilibrium critical thickness curves.[4,5] Unfortunately, these equilibrium theories completely leave out the question of whether the desired minimum energy state is kinetically accessible.

In order to address the latter question, it is necessary to know *how* the sample relaxes, i.e., to identify the precise microscopic mechanisms involved, to understand how these mechanisms interact to result in the overall process, and how the epitaxial microstructure affects these mechanisms. For example, the appearance of strain relieving, interfacial misfit dislocations requires some sequence of processes, such as surface nucleation of dislocation half-loops, multiplication, and glide of the threading segments.[10] Some or all of these might have some characteristic thermal activation which may dominate within a particular range of temperatures. For instance, glide of dislocations in bulk Si is a thermally activated process with a (possibly strain dependent[10]) activation energy near 2 eV[16] while generation mechanisms, which at this point are not well understood in this system, may have a significantly lower activation energy (< 1 eV).[17] Steps in this direction have been taken in a recent set of papers by Dodson and co-workers.[10,18–20] In their work, an attempt is made to account for the observed metastable behavior through a phenomenological description of thermally activated microscopic processes such as dislocation nucleation, glide, etc., which must act in the proper sequence to result in the stable, relaxed configuration.

We can attempt to determine what microscopic processes are significant on the basis of our observations. For example, in Sec. III we saw that our coherently strained superlattice sample relaxed to a significantly lesser extent than a corresponding alloy sample as a result of a 700 °C, 2 h anneal. This result suggests that additional kinetic barriers are present in the superlattice which are absent in the alloy. For instance, it is well known that superlattices can be effective as dislocation-blocking filters in lattice-mismatched heteroepitaxy as in the growth of GaAsP on GaAs.[21] In that case, it is believed that the alternating strain fields in the superlattice interfere with the propagation of dislocations upward across layer interfaces, causing the dislocations instead to bend laterally outward to the sides of the crystal. In the present work, strain relaxation may be taking place through some surface nucleation and glide processes as mentioned above. If this is indeed the case, then our results suggest that the movement of dislocations is being hindered by the alternating strain fields of the superlattice. Our results would further tend to rule out any mechanisms which do *not* involve the movement of dislocation lines across superlattice interfacial layers since in such a case one would expect to have the same relaxation behavior in both the superlattice and alloy films. At this point, it is important to note that the differing extent of relaxation observed for alloys and superltices is only apparent; the true final relaxed state of both structures is similar, but the superlattice gets "trapped" in a metastable, incompletely relaxed configuration.

Another significant aspect of the present work is the fact that we observe strain relaxation at temperatures as low as 390 °C. That we get appreciable activation at such a low temperature is apparently due to the significant amount of excess stress[10] "frozen" into our structures since they are grown so far in excess of the equilibrium critical thickness. It is possible that the large excess stress results in a lower effective kinetic barrier because of the large "driving force" associated with the stress. For example, as the thickness is lessened to a value below the People and Bean critical thickness[2] (but still above the equilibrium critical thickness), the films will appear coherently strained at least up to 550 °C (the growth temperatures usually employed for $Si_{1-x}Ge_x$ MBE layers). However, recent work by Baribeau *et al.*[15] shows that such samples may relax upon heating to still greater temperatures. Thus, it would appear that the rate of strain relaxation, for a given *type* of structure, increases with increasing film thickness (increasing excess stress). The systematics of this dependence on film thickness and composition remain to be explored.

Recently, there has been related work on the subject of strain relaxation in $Si_{1-x}Ge_x/Si$ heterostructures. Tuppen *et al.* have shown that alternating strain fields between the layers of a $Si_{1-x}Ge_x/Si$ superlattice interfere with the glide of dislocation half-loops.[8] These workers use this observation to account for the difference in apparent extent of relax-

ation between $Si_{1-x}Ge_x$ superlattices and single alloy layers. This conclusion is consistent with the results of the present study. However, it is interesting to note that Tuppen *et al.* reached their conclusion from strain measurements made over a set of several samples which were grown at substantially higher temperature (550–600 °C) and over a range of film thicknesses both above and below the People and Bean critical thickness,[2] whereas in the present work, the same conclusion is reached by directly observing the extent of strain relaxation in initially strained superlattices and alloys.

There have also been other *ex situ* anneal experiments reported recently for $Si_{1-x}Ge_x$ single alloy layers. Fiory *et al.* have studied strain relaxation in $Si_{1-x}Ge_x$ films through ion channeling and TEM observations.[22] More recently, Hull has reported on strain relaxation dynamics based on real-time observation of *in situ*-annealed TEM specimens.[23] Also, Baribeau *et al.* have made XRD measurements of *ex situ*-annealed alloy and superlattice films, as mentioned above.[15] However, in all of these cases, the films were grown near 550 °C and at or below the People and Bean critical thickness,[2] and the *ex situ* anneals had to be performed at much higher temperatures (~ 800 °C or more) in order to observe substantial relaxation effects. It is quite possible that, at such high anneal temperatures, the strain relaxation kinetics is governed by a different rate-limiting behavior, and that the dominant relaxation mechanism(s) may be different. Moreover, the effects of bulk interdiffusion at heterojunction interfaces can no longer be neglected at these temperatures. In order to better understand the microscopic behavior during strain relaxation in our own samples, we are presently attempting TEM measurements and will report the results in a later publication.[24]

V. CONCLUSIONS

In conclusion, we have studied the strain relaxation in initially strained $Si_{1-x}Ge_x/Si$ heteroepitaxial structures through *ex situ* anneal treatment with the use of x-ray diffraction and Raman spectroscopic techniques. Highly strained samples are produced through molecular-beam epitaxial growth at unusually low temperature (≈ 365 °C). This results in nearly coherently strained, metastable alloy and superlattice structures grown significantly in excess of critical thicknesses previously reported for such structures. These samples readily relax their strains upon subsequent anneals at temperatures ranging from 390 to 450 °C, substantially below the *growth* temperatures typically employed in similar strain relaxation studies of this material system. The *extent* of strain relaxation after a 700 °C, 2 h anneal is seen to differ for single $Si_{1-x}Ge_x$ layers and corresponding $Si_{1-x}Ge_x/Si$ superlattices of the same total thickness and average alloy composition. The strain relaxation kinetics of an initially strained alloy layer is studied quantitatively for the first time. Strain relaxation in this case is seen to be approximately described by a single, thermally activated, first order kinetic process having activation energy $E_a = 2.0$ eV. This value is close to the activation energy associated with dislocation motion through glide in bulk Si. Such a quantitative analysis should prove useful in identifying the relevant

microscopic mechanisms responsible for strain relaxation in lattice-mismatched semiconductor heterostructures.

ACKNOWLEDGMENTS

[a] Present address: Department of Materials Science and Engineering, Stanford University, Palo Alto, CA 94305.

[1] J. C. Bean, L. C. Feldman, A. T. Fiory, S. Nakahara, and I. K. Robinson, J. Vac. Sci. Technol. A **2**, 436 (1984).

[2] R. People and J. C. Bean, Appl. Phys. Lett. **47**, 322 (1985); Appl. Phys. Lett. **49**, 229 (1986).

[3] R. Hull, J. C. Bean, F. Cerdeira, A. T. Fiory, and J. M. Gibson, Appl. Phys. Lett. **48**, 56 (1986).

[4] J. H. Van der Merwe, J. Appl. Phys. **34**, 123 (1962).

[5] J. W. Matthews and A. E. Blakeslee, J. Cryst. Growth **27**, 118 (1974).

[6] R. H. Miles, T. C. McGill, P. P. Chow, D. C. Johnson, R. J. Hauenstein, C. W. Nieh, and M. D. Strathman, Appl. Phys. Lett. **52**, 916 (1988).

[7] R. H. Miles, P. P. Chow, D. C. Johnson, R. J. Hauenstein, O. J. Marsh, C. W. Nieh, M. D. Strathman, and T. C. McGill, J. Vac. Sci. Technol. B **6**, 1382 (1988).

[8] C. G. Tuppen, C. J. Gibbings, S. T. Davey, M. H. Lyons, M. Hockly, and M. A. G. Halliwell, in *Proceedings of the Second International Symposium on Silicon Molecular Beam Epitaxy*, edited by J. C. Bean and L. J. Schowalter (The Electrochemical Society, Pennington, 1988), p. 36.

[9] E. Kasper, *Festkörperprobleme (Advances in Solid State Physics)*, edited by P. Grosse (Viewag, Braunschweig, 1987), Vol. 27, p. 265.

[10] B. W. Dodson and J. Y. Tsao, Appl. Phys. Lett. **51**, 1325 (1987).

[11] C. F. Huang, R. P. G. Karunasiri, K. L. Wang, and T. W. Kang, in *Proceedings of the Second International Symposium on Silicon Molecular Beam Epitaxy*, edited by J. C. Bean and L. J. Schowalter (The Electrochemical Society, Pennington, 1988), p. 501

[12] D. Striet and F. Allen, J. Appl. Phys. **61**, 2894 (1987).

[13] This assumes a linear interpolation with composition of elastic constants between those of pure Si and Ge, and neglects the contributions of higher order elastic constants, which can be shown to be negligible for the present situation.

[14] E. Anastassakis, A. Pinczuk, and E. Burstein, Solid State Commun. **8**, 133 (1970).

[15] J.-M. Baribeau, S. Kechang, and K. Munro, Appl. Phys. Lett. **54**, 323 (1989).

[16] L. B. Freund, A. Bower, and J. C. Ramirez, MRS Fall Meeting, Boston, 1988.

[17] B. W. Dodson (private communication).

[18] B. W. Dodson and J. Y. Tsao, Phys. Rev. B **38**, 12383, (1988).

[19] B. W. Dodson, Appl. Phys. Lett. **53**, 394 (1988).

[20] J. Y. Tsao and B. W. Dodson, Appl. Phys. Lett. **53**, 848 (1988).

[21] J. W. Matthews, A. E. Blakeslee, and S. Mader, Thin Solid Films **33**, 253 (1976).

[22] A. T. Fiory, J. C. Bean, R. Hull, and S. Nakahara, Phys. Rev. B **31**, 4063 (1984).

[23] R. Hull, J. C. Bean, D. J. Werder, and R. E. Leibenguth, Appl. Phys. Lett. **52**, 1605 (1988).

[24] R. J. Hauenstein, R. H. Miles, E. T. Croke, C. W. Neih, and T. C. McGill (to be published).